A Predictive Model for the Excess Gibbs Free Energy of Fully Dissociated Electrolyte Solutions

Meng-Ting Hsieh and Shiang-Tai Lin
Dept. of Chemical Engineering, National Taiwan University, Taipei, Taiwan 10617, Taiwan

DOI 10.1002/aic.12325
Published online July 19, 2010 in Wiley Online Library (wileyonlinelibrary.com).

In this work, we show that the mean activity coefficient, osmotic coefficient, and vapor pressure of aqueous electrolyte solutions can be successfully predicted through combining the Pitzer-Debye-Hückel model for long-range interactions and the modified COSMO-SAC model for short-range interactions. This method contains only a small number (13) of universal parameters to describe various types of interactions between different species, such as ions, hydrogen-bonding species, and non-hydrogen bonding species. This approach does not require any pair interaction parameters between species and does not contain any ion specific parameter other than the element radius. We have examined this method for the properties of three types of systems, including a single salt in water, mixture salts in water, and a single salt in solvent mixtures containing water and alcohols. The predicted results are found to be in good agreement with those from experiments over wide ranges of concentration and temperature. This model is, in principle, applicable to all types of electrolyte solutions and is especially useful for property estimation for cases when no experimental data are available.
 AIChE J, 57: 1061–1074, 2011
Keywords: electrolyte, mean activity coefficient, osmotic coefficient, Pitzer-Debye-Hückel, COSMO-SAC

Introduction

Electrolyte solutions are frequently encountered in natural systems, such as sea water and biological systems, as well as in chemical and pharmaceutical industries.[1,2] However, describing the thermodynamic properties of electrolyte solutions using conventional thermodynamic models has been quite challenging. This can be easily understood through the generalized van der Waals theory.[3,4] The long-range interactions, which is important between charged species in electrolyte solutions, are neglected in most engineering liquid models, such as NRTL,[5] UNIQUAC,[6] and UNIFAC,[7] and equations of state, such as the Peng-Robinson,[8] SAFT,[9] and PC-SAFT[10] EOS. One common remedy for such a deficiency is to add a long-range correction to the existing (short range) models. For example, the excess Gibbs free energy

$$\underline{G}^{\mathrm{ex}} = \underline{G}^{\mathrm{ex,LR}} + \underline{G}^{\mathrm{ex,SR}} \tag{1}$$

where the long-range corrections are based either on the (modified) Debye-Hückel (DH) model[11] or the mean spherical approximation (MSA).[12] Both the DH and MSA theory provide an accurate description of the non-ideality in dilute aqueous electrolyte solutions where ions are completely solvated by water molecules. However, as the concentration of electrolyte increases, ionic species may start coming into contact and the short-range interactions become important.

The separate consideration of long-range and short-range interactions has lead to many successful correlative or

Correspondence concerning this article should be addressed to S.-T. Lin at stlin@ntu.edu.tw.

semi-predictive models. For example, the electrolyte-NRTL model[13–16] uses the Pitzer Debye-Hückel (PDH)[17] for long-range contribution and the non-random-two-liquid (NRTL) model[5] for the short-range contributions. In the two ionic parameter model,[18,19] the PDH model is combined with a solvation effect term. In the IP-MGV-MSA model,[20] the MSA theory is used to account for long-range interactions whereas the modified Ghotbi-Vera Hard sphere model[21] is used for short-range interactions. Jin and Donohue[22–24] used the PACT[25] (perturbed anisotropic chain theory) EOS for short-range interaction and a perturbation expansion of Henderson and Blum's restricted primitive model[26] for long-range charge–charge interactions. Fürst and Renon[27] developed an EOS which combines the EOS of Schwartzentruber et al.[28] with MSA. Myers et al.[29,30] combine the PR EOS with MSA to describe the behavior of aqueous electrolyte solutions over a wide range of temperature and pressure.

Despite the success of these models in modeling the thermodynamic properties of electrolyte solutions, they usually contain salt-dependent parameters whose value must be determined via fitting to the experimental data of the electrolyte solution of interest. Such a type of models cannot be used to predict the properties of a solution that contains a new salt species. (For example, the parameters determined from NaCl aqueous solution are not of any use for the solution of NaBr). Recently, Held et al.[31] proposed an ePC-SAFT EOS,[32] which combines the DH model and PC-SAFT EOS, that requires only two characteristic parameters for each ionic species. The value of these characteristic parameters does not change whether an ionic species (e.g., Na^+) is in one salt (e.g., NaCl) or in another (e.g., NaBr). The use of ion-specific parameters (instead of salt-specific parameters) greatly enhances the predictive power of the ePC-SAFT EOS for new electrolyte solutions. Nonetheless, the characteristic parameters of each new ionic species must be determined with experimental data.

The main objective of the present work is to develop a model for electrolyte solutions that does not contain any species-specific parameters. This is made possible by combining the PDH model[17] with a predictive activity coefficient model, COSMO-SAC.[33] This approach requires a small group (13) of universal parameters to describe the specific interactions between charged-charged, charged-neutral, and/or neutral-neutral species. The resultant model is, in principle, applicable to all types of electrolyte systems and can provide reliable predictions of mean activity coefficient, osmotic coefficient, and vapor pressure of various types of electrolyte solutions (e.g., single-salt single-solvent, mixed-salt single-solvent, and single-salt mixed-solvent).

Theory

The system of our interest here is a solution containing completely dissociated electrolytes and solvents. For example, a solution containing n_A moles of ion A (with a net charge of z_A), n_B moles of ion B (with a net charge of z_B), n_C moles of ion C (with a net charge of z_C),…, n_{S1} moles of solvent 1, and n_{S2} moles of solvent 2 can be represented as

$$n_A A^{z_A} + n_B B^{z_B} + n_C C^{z_C} + \cdots + n_{S1}\text{Solvent1} + n_{S2}\text{Solvent2} \tag{2}$$

Electrical neutrality requires the following relation be always satisfied

$$n_A z_A + n_B z_B + n_C z_C + \cdots = \sum_i n_i z_i = 0 \tag{3}$$

where the summation for i(=A,B,C,…,Solvent1,Solvent2) is over all species in the solution, and z_i is the charge of species i ($z_i = 0$ for the solvents). The molar Gibbs free energy of the solution at temperature T, pressure P, and composition x, can be expressed as the sum of the partial molar Gibbs free energy of each species in the system, that is,

$$\underline{G}(T,P,\underline{x}) = \sum_i x_i \bar{G}_i(T,P,\underline{x}) \tag{4}$$

where x_i is the mole fraction of each species. The molar excess Gibbs free energy of such a mixture is

$$\underline{G}^{ex} = \underline{G} - \sum_i x_i \bar{G}_i^o = \underline{G}^{ex,PHD} + \underline{G}^{ex,COSMOSAC} \tag{5}$$

where $\bar{G}_i^o$ is the partial molar Gibbs free energy of i at some reference state. The last equality follows from Eq. 1 where $\underline{G}^{ex}$ is decomposed to a long-range effect, described here using the Pitzer Debye-Hückel (PDH) theory, and a short-range effect, described using a modified COSMO-SAC model. The activity coefficient is thus obtained as

$$\ln \gamma_i = \frac{1}{RT}\left(\frac{\partial n\underline{G}^{ex}}{\partial n_i}\right)_{T,P,n_{j\neq i}} = \ln \gamma_i^{PDH} + \ln \gamma_i^{COSMOSAC} \tag{6}$$

where n is the total number of moles. The activity coefficient equation from PDH theory and the COSMO-SAC model is presented as follows.

The Pitzer Debye-Hückel theory

The unsymmetric PDH formula[17] describes the molar excess Gibbs free energy as

$$\frac{\underline{G}^{ex,PDH}}{RT} = -\left(\frac{1000}{M_s}\right)^{1/2} A_\phi \left(\frac{4I_x}{\rho}\right) \ln\left(1 + \rho I_x^{1/2}\right) \tag{7}$$

where M_s is the average molecular weight of solvent, ρ is the closest approach parameter, I_x is the ionic strength

$$I_x = \frac{1}{2}\sum_i x_i z_i^2 \tag{8}$$

and A_ϕ is the Debye-Hückel constant defined as

$$A_\phi = \frac{1}{3}\left(\frac{2\pi N_A d_s}{1000}\right)^{1/2}\left(\frac{Q_e^2}{\varepsilon_s kT}\right)^{3/2} \tag{9}$$

with d_s being the density of solvent, N_A the Avogadro's number, Q_e the charge of an electron, ε_s the average dielectric of solvent, and k the Boltzmann constant. Note that the word "unsymmetric" represents the fact that a different reference state for ionic and neutral species in Eq. 7. For ionic species, the reference state is in infinite-dilution solution (i.e., $\bar{G}_i^o(T,P,x_i = 0)$). However, the reference state for solvent is defined in its pure liquid state (i.e., $\bar{G}_i^o(T,P,x_i = 1)$).

The activity coefficient of each species can be derived from Eq. 7

$$\ln \gamma_i^{PDH} = -\left(\frac{1000}{M_s}\right)^{1/2} A_\phi \left[\left(\frac{2z_i^2}{\rho}\right)\ln\left(1+\rho I_x^{1/2}\right) + \frac{z_i^2 I_x^{1/2} - 2I_x^{3/2}}{1+\rho I_x^{1/2}}\right] \quad (10)$$

Equation 10 is used for the long-range effect on the activity coefficient.

While Eq. 10 was derived for the case of a single-solvent solution, Chen and Song suggest[34] that it can be extended to multi-solvent systems by considering the neutral components as one pseudo-single-solvent. The properties of such a pseudo-single-solvent is determined according to the following simple mixing rule

$$M_s = \sum_k x'_k M_k \quad (11)$$

$$\frac{1}{d_s} = \sum_k \frac{x'_k}{d_k} \quad (12)$$

$$\varepsilon_s = \sum_k w'_k \varepsilon_k \quad (13)$$

where M_s, d_s, and ε_s are the properties of the pseudo-single-solvent and can be applied to Eq. 10 directly. M_k, d_k, and ε_k are the properties of solvent component k, and the summation runs over all solvent components (i.e., all the neutral species) in the solution. The x'_k and w'_k are the ion-free mole fraction and average molecular weight

$$x'_k = \frac{x_k}{\sum_j x_j} \quad (14)$$

$$w'_k = \frac{M_k x_k}{\sum_j x_j M_j} \quad (15)$$

where the summations in Eqs. 14 and 15 are over all the solvent species in the solution. Note that the temperature dependence of the density and the dielectric constant of pure water is considered in this work. The equation suggested by Novotny and Sohnel[35] is used for the density

$$d_w = 999.65 + 0.20438\cdot(T-273.15) - 0.06174\cdot(T-273.15)^{3/2} \quad (16)$$

and the following semi-empirical equation[36] is used for the dielectric constant

$$\varepsilon_w = 3.84093\cdot 10^{-4}\cdot(T-298.15)^2 - 3.18404\cdot 10^{-1}\cdot(T-298.15) + 78.3055 \quad (17)$$

The COSMO-SAC model[33]

The effect of short-range interactions on the activity coefficient is described by the COSMO-SAC model, in which the attractive (residual) and repulsive (combinatorial) interactions are considered separately as

$$\ln \gamma_i^{COSMOSAC} = \ln \gamma_i^{res} + \ln \gamma_i^{comb} \quad (18)$$

In the residual component, the interactions at the contacting surface between two species can be determined from the surface screening charges determined when the species is solvated in a perfect conductor.

$$\ln \gamma_i^{res} = n_i \sum_{\sigma_m} p_i(\sigma_m)\ln[\Gamma_S(\sigma_m) - \Gamma_i(\sigma_m)] \quad (19)$$

where the sigma profile $p_i(\sigma_m)$ is the probability of finding a surface of charge density σ_m on species i. The value n_i is the number of surface segments of species i calculated from the ratio of the molecular surface area A_i and the effective area of surface contact a_{eff}, that is, $n_i = A_i/a_{eff}$. The segment activity coefficient Γ is calculated from

$$\ln \Gamma_k(\sigma_m) = -\ln\left\{\sum_{\sigma_n} p_k(\sigma_n)\Gamma_k(\sigma_n)\exp\left[\frac{-\Delta W(\sigma_m,\sigma_n)}{kT}\right]\right\} \quad (20)$$

where the subscript k can either be the solution S or the pure species i. $\Delta W(\sigma_m,\sigma_n)$ is the interaction between segments m and n (each has characterized with its charge density σ_m,σ_n, respectively) and will be described in detail later.

The Staverman-Guggenheim (SG) model is used for the combinatorial term

$$\ln \gamma_i^{comb} = \ln\frac{\phi_i}{x_i} + \frac{z}{2}q_i\ln\frac{\theta_i}{\phi_i} + l_i - \frac{\phi_i}{x_i}\sum_j x_j l_j \quad (21)$$

where $z = 10$ is the coordination number, r_i and q_i are the normalized volume and surface area, $\theta_i = \frac{x_i q_i}{\sum_j x_j q_j}$ is the surface fraction $\phi_i = \frac{x_i r_i}{\sum_j x_j r_j}$ is the volume fraction, and $l_i = \frac{z}{2}(r_i - q_i) - (r_i - 1)$.

Specific interactions in electrolyte solutions

To take into account the specific interactions between ion and solvent, and between ion and ion, the sigma profile of each species is considered to have four components: the electrostatic (non-hydrogen bonding) segments (nonhb), the hydrogen-bonding segments (hb), the ionic segments(ion), and the ionic group segments (iongrp), that is,

$$p_i(\sigma_m) = p_i^{nonhb}(\sigma_m^{nonhb}) + p_i^{hb}(\sigma_m^{hb}) + p_i^{ion}(\sigma_m^{ion}) + p_i^{iongrp}(\sigma_m^{iongrp}) \quad (22)$$

Hydrogen-bonding segments are those from the surface of HB donating (e.g., H in H_2O) or accepting (e.g., O in H_2O) atoms. Ionic segments are those from the surfaces of charged atoms, such as Na^+, Ca^{2+}, Cl^-, Br^-, etc. Ionic group segments are the surfaces of charged molecules, such as NH_4^+, NO_3^-, etc. All other segments are classified as non-hydrogen bonding segments. Because of such changes in the sigma-profile, there are 10 (=(1+4)×4/2) possible types of interactions as illustrated in Figure 1. To reflect the fact that, for example, the strength of interaction between a cation with water is different from that between an anion and water, the

HB-ion interactions is decomposed further to four sub-categories, HB donor-anion, HB donor-cation, HB acceptor-anion, and HB acceptor-cation. Such refinement is done also for HB-HB, Ion-Ion, Ion group-Ion group, HB-ion group, Ion-ion group interactions. Table 1 summarizes the all possible interactions considered in this work. To include all these effects, Eqs. 19 and 20 become[37]

$$\ln \gamma_{\mathrm{i}}^{\mathrm{res}} = n_{\mathrm{i}} \sum_{\mathrm{s}}^{\substack{\mathrm{nonhb,hb,}\\ \mathrm{ion,iongrp}}} \sum_{\sigma_{\mathrm{m}}} p_{\mathrm{i}}^{\mathrm{s}}(\sigma_{\mathrm{m}}) \ln\left[\Gamma_{\mathrm{S}}^{\mathrm{s}}(\sigma_{\mathrm{m}}^{\mathrm{s}}) - \Gamma_{\mathrm{i}}^{\mathrm{s}}(\sigma_{\mathrm{m}}^{\mathrm{s}})\right] \quad (23)$$

$$\ln \Gamma_{\mathrm{j}}^{t}(\sigma_{\mathrm{m}}^{t}) = -\ln\left\{ \sum_{\mathrm{s}}^{\substack{\mathrm{nonhb,hb,}\\ \mathrm{ion,iongrp}}} \sum_{\sigma_{\mathrm{n}}} p_{\mathrm{j}}^{\mathrm{s}}(\sigma_{\mathrm{n}}^{\mathrm{s}}) \exp\left[\frac{-\Delta W(\sigma_{\mathrm{m}}^{\mathrm{t}}, \sigma_{\mathrm{n}}^{\mathrm{s}})}{kT} + \ln \Gamma_{\mathrm{j}}^{\mathrm{s}}(\sigma_{\mathrm{n}}^{\mathrm{s}})\right]\right\} \quad (24)$$

where the subscript j is either the pure fluid i or the solvent S, and the segment interaction energy $\Delta W(\sigma_{\mathrm{m}}^{\mathrm{t}}, \sigma_{\mathrm{n}}^{\mathrm{s}})$ is described as

$$\Delta W(\sigma_{\mathrm{m}}^{\mathrm{t}}, \sigma_{\mathrm{n}}^{\mathrm{s}}) = \begin{cases} a_0(\sigma_{\mathrm{m}}^{\mathrm{t}} + \sigma_{\mathrm{n}}^{\mathrm{s}})^2 & \text{if}(\mathrm{t} = \mathrm{nonhb\ or\ s} = \mathrm{nonhb}) \\ & \text{or}\ (\mathrm{t} = \mathrm{s} = \mathrm{hb\ and}\ \sigma_{\mathrm{m}}^{\mathrm{t}} \cdot \sigma_{\mathrm{n}}^{\mathrm{s}} > 0) \quad \text{(a)} \\ a_0(\sigma_{\mathrm{m}}^{\mathrm{t}} + \sigma_{\mathrm{n}}^{\mathrm{s}})^2 - b_0(\sigma_{\mathrm{m}}^{\mathrm{t}} - \sigma_{\mathrm{n}}^{\mathrm{s}})^2 & \text{if}(\mathrm{t} = \mathrm{s} = \mathrm{hb\ and}\ \sigma_{\mathrm{m}}^{\mathrm{t}} \cdot \sigma_{\mathrm{n}}^{\mathrm{s}} < 0) \quad \text{(b)} \\ a_1(\sigma_{\mathrm{m}}^{\mathrm{t}} + \sigma_{\mathrm{n}}^{\mathrm{s}})^2 & \text{if}(\mathrm{t} = \mathrm{s} = \mathrm{ion}, \sigma_{\mathrm{m}}^{\mathrm{t}} > 0, \text{ and } \sigma_{\mathrm{n}}^{\mathrm{s}} > 0) \\ & \text{or}\ (\mathrm{t} = \mathrm{s} = \mathrm{iongrp}, \sigma_{\mathrm{m}}^{\mathrm{t}} > 0, \text{ and } \sigma_{\mathrm{n}}^{\mathrm{s}} > 0) \\ & \text{or}\ (\mathrm{t} = \mathrm{ion, s} = \mathrm{iongrp}, \sigma_{\mathrm{m}}^{\mathrm{t}} > 0, \text{ and } \sigma_{\mathrm{n}}^{\mathrm{s}} > 0) \\ & \text{or}\ (\mathrm{t} = \mathrm{iongrp, s} = \mathrm{ion}, \sigma_{\mathrm{m}}^{\mathrm{t}} > 0, \text{ and } \sigma_{\mathrm{n}}^{\mathrm{s}} > 0) \quad \text{(c)} \\ a_2(\sigma_{\mathrm{m}}^{\mathrm{t}} + \sigma_{\mathrm{n}}^{\mathrm{s}})^2 & \text{if}(\mathrm{t} = \mathrm{s} = \mathrm{ion}, \sigma_{\mathrm{m}}^{\mathrm{t}} < 0, \text{ and } \sigma_{\mathrm{n}}^{\mathrm{s}} < 0) \\ & \text{or}\ (\mathrm{t} = \mathrm{s} = \mathrm{iongrp}, \sigma_{\mathrm{m}}^{\mathrm{t}} < 0, \text{ and } \sigma_{\mathrm{n}}^{\mathrm{s}} < 0) \\ & \text{or}\ (\mathrm{t} = \mathrm{ion, s} = \mathrm{iongrp}\ \sigma_{\mathrm{m}}^{\mathrm{t}} < 0, \text{ and } \sigma_{\mathrm{n}}^{\mathrm{s}} < 0) \\ & \text{or}\ (\mathrm{t} = \mathrm{iongrp, s} = \mathrm{ion}, \sigma_{\mathrm{m}}^{\mathrm{t}} < 0, \text{ and } \sigma_{\mathrm{n}}^{\mathrm{s}} < 0) \quad \text{(d)} \\ a_3(\sigma_{\mathrm{m}}^{\mathrm{t}} + \sigma_{\mathrm{n}}^{\mathrm{s}})^2 & \text{if}(\mathrm{t} = \mathrm{s} = \mathrm{ion\ and}\ \sigma_{\mathrm{m}}^{\mathrm{t}} \cdot \sigma_{\mathrm{n}}^{\mathrm{s}} < 0) \quad \text{(e)} \\ a_4(\sigma_{\mathrm{m}}^{\mathrm{t}} + \sigma_{\mathrm{n}}^{\mathrm{s}})^2 & \text{if}(\mathrm{t} = \mathrm{s} = \mathrm{iongrp}, \text{ and } \sigma_{\mathrm{m}}^{\mathrm{t}} \cdot \sigma_{\mathrm{n}}^{\mathrm{s}} < 0) \\ & \text{or}\ (\mathrm{t} = \mathrm{ion, s} = \mathrm{iongrp}, \text{ and } \sigma_{\mathrm{m}}^{\mathrm{t}} \cdot \sigma_{\mathrm{n}}^{\mathrm{s}} < 0) \\ & \text{or}\ (\mathrm{t} = \mathrm{iongrp, s} = \mathrm{ion}, \text{ and } \sigma_{\mathrm{m}}^{\mathrm{t}} \cdot \sigma_{\mathrm{n}}^{\mathrm{s}} < 0) \quad \text{(f)} \\ a_5(\sigma_{\mathrm{m}}^{\mathrm{t}} + \sigma_{\mathrm{n}}^{\mathrm{s}})^2 - b_1(\sigma_{\mathrm{m}}^{\mathrm{t}} - \sigma_{\mathrm{n}}^{\mathrm{s}})^{2.5} & \text{if}(\mathrm{t} = \mathrm{hb, s} = \mathrm{ion}, \sigma_{\mathrm{m}}^{\mathrm{t}} < 0 \text{ and } \sigma_{\mathrm{n}}^{\mathrm{s}} > 0) \\ & \text{or}\ (\mathrm{t} = \mathrm{ion, s} = \mathrm{hb}, \sigma_{\mathrm{m}}^{\mathrm{t}} > 0 \text{ and } \sigma_{\mathrm{n}}^{\mathrm{s}} < 0) \quad \text{(g)} \\ a_6(\sigma_{\mathrm{m}}^{\mathrm{t}} + \sigma_{\mathrm{n}}^{\mathrm{s}})^2 & \text{if}(\mathrm{t} = \mathrm{hb, s} = \mathrm{ion}, \sigma_{\mathrm{m}}^{\mathrm{t}} < 0, \text{ and } \sigma_{\mathrm{n}}^{\mathrm{s}} < 0) \\ & \text{or}\ (\mathrm{t} = \mathrm{ion, s} = \mathrm{hb}, \sigma_{\mathrm{m}}^{\mathrm{t}} < 0, \text{ and } \sigma_{\mathrm{n}}^{\mathrm{s}} < 0) \\ & \text{or}\ (\mathrm{t} = \mathrm{hb, s} = \mathrm{iongrp}, \sigma_{\mathrm{m}}^{\mathrm{t}} < 0, \text{ and } \sigma_{\mathrm{n}}^{\mathrm{s}} < 0) \\ & \text{or}\ (\mathrm{t} = \mathrm{iongrp, s} = \mathrm{hb}, \sigma_{\mathrm{m}}^{\mathrm{t}} < 0, \text{ and } \sigma_{\mathrm{n}}^{\mathrm{s}} < 0) \quad \text{(h)} \\ a_7(\sigma_{\mathrm{m}}^{\mathrm{t}} + \sigma_{\mathrm{n}}^{\mathrm{s}})^2 & \text{if}(\mathrm{t} = \mathrm{hb, s} = \mathrm{ion}, \sigma_{\mathrm{m}}^{\mathrm{t}} > 0, \text{ and } \sigma_{\mathrm{n}}^{\mathrm{s}} > 0) \\ & \text{or}\ (\mathrm{t} = \mathrm{ion, s} = \mathrm{hb}, \sigma_{\mathrm{m}}^{\mathrm{t}} > 0, \text{ and } \sigma_{\mathrm{n}}^{\mathrm{s}} > 0) \quad \text{(i)} \\ a_5(\sigma_{\mathrm{m}}^{\mathrm{t}} + \sigma_{\mathrm{n}}^{\mathrm{s}})^2 - b_2(\sigma_{\mathrm{m}}^{\mathrm{t}} - \sigma_{\mathrm{n}}^{\mathrm{s}})^{2.5} & \text{if}(\mathrm{t} = \mathrm{hb, s} = \mathrm{ion}, \sigma_{\mathrm{m}}^{\mathrm{t}} > 0, \text{ and } \sigma_{\mathrm{n}}^{\mathrm{s}} < 0) \\ & \text{or}\ (\mathrm{t} = \mathrm{ion, s} = \mathrm{hb}, \sigma_{\mathrm{m}}^{\mathrm{t}} < 0, \text{ and } \sigma_{\mathrm{n}}^{\mathrm{s}} > 0) \\ & \text{or}\ (\mathrm{t} = \mathrm{hb, s} = \mathrm{iongrp}, \sigma_{\mathrm{m}}^{\mathrm{t}} > 0 \text{ and } \sigma_{\mathrm{n}}^{\mathrm{s}} < 0) \\ & \text{or}\ (\mathrm{t} = \mathrm{iongrp, s} = \mathrm{hb}, \sigma_{\mathrm{m}}^{\mathrm{t}} < 0 \text{ and } \sigma_{\mathrm{n}}^{\mathrm{s}} > 0) \quad \text{(j)} \\ -a_8(\sigma_{\mathrm{m}}^{\mathrm{t}} + \sigma_{\mathrm{n}}^{\mathrm{s}})^2 & \text{if}(\mathrm{t} = \mathrm{hb, s} = \mathrm{iongrp}, \sigma_{\mathrm{m}}^{\mathrm{t}} < 0, \text{ and } \sigma_{\mathrm{n}}^{\mathrm{s}} > 0) \\ & \text{or}\ (\mathrm{t} = \mathrm{iongrp, s} = \mathrm{hb}, \sigma_{\mathrm{m}}^{\mathrm{t}} > 0, \text{ and } \sigma_{\mathrm{n}}^{\mathrm{s}} < 0) \quad \text{(k)} \\ a_9(\sigma_{\mathrm{m}}^{\mathrm{t}} + \sigma_{\mathrm{n}}^{\mathrm{s}})^2 & \text{if}(\mathrm{t} = \mathrm{hb, s} = \mathrm{iongrp}, \sigma_{\mathrm{m}}^{\mathrm{t}} > 0, \text{ and } \sigma_{\mathrm{n}}^{\mathrm{s}} > 0) \\ & \text{or}\ (\mathrm{t} = \mathrm{iongrp, s} = \mathrm{hb}, \sigma_{\mathrm{m}}^{\mathrm{t}} > 0, \text{ and } \sigma_{\mathrm{n}}^{\mathrm{s}} > 0) \quad \text{(l)} \end{cases} \quad (25)$$

Note that Eqs. 25a and b have been used in the original COSMO-SAC model[33] for interactions between neutral species. Here, we have introduced 10 additional empirical Eqs. 25c–l, containing 11 universal parameters (a_1 to a_9, b_1 and b_2 whose values were determined from fitting to experimental data) to properly describe the interactions between ionic species and the solvent. The values of all these parameters are summarized in Table 2.

Computational Details

Activity coefficient from PDH model

The physical properties of the solvent (density, molecular weight) are taken from the DIPPR database[38] and the dielectric constant from Chen and Song.[39] In the case of water, the value of density and dielectric constant are calculated from Eqs. 16 and 17. For mixed-solvent systems, the pseudo-single solvent properties are determined from Eqs. 11 to 13. These properties are used to determine the

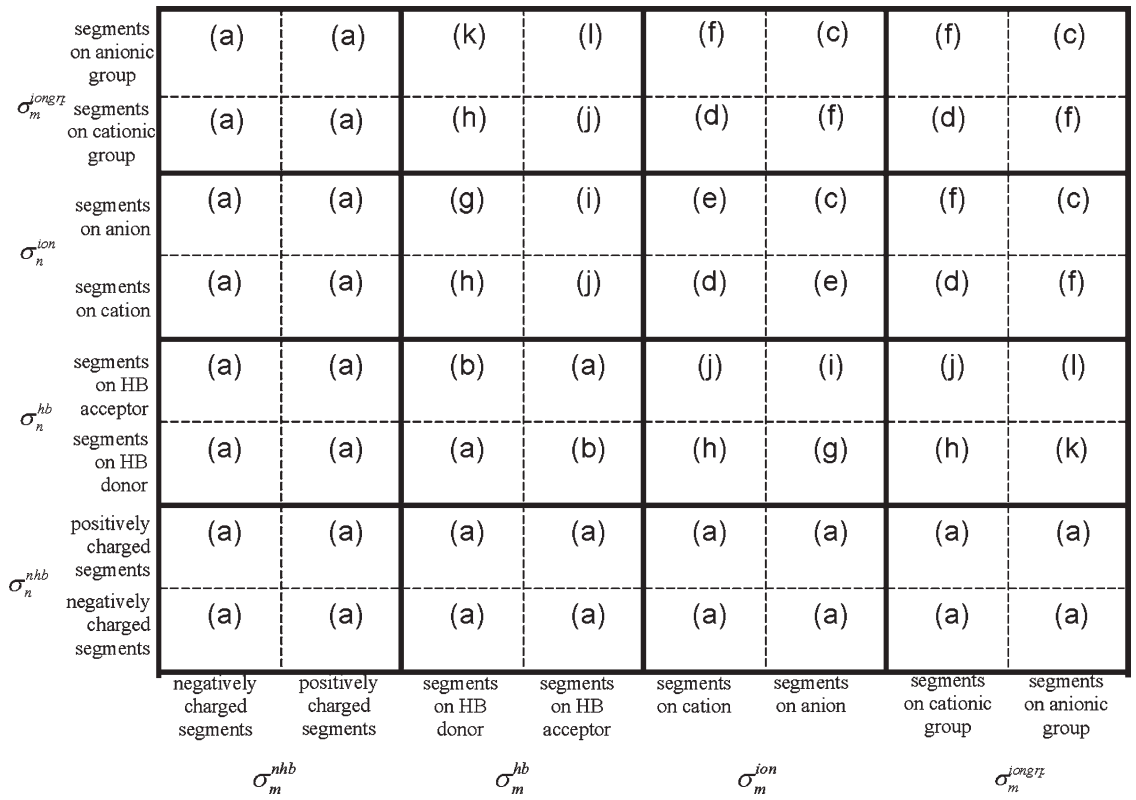

Figure 1. Illustration of $\Delta W(\sigma_m,\sigma_n)$ between different segment types.

The letters in parenthesis indicates the corresponding equation in Eq. 25.

Debye-Hückel constant A_ϕ in Eq. 9. The closest approach parameter ρ is estimated using the following empirical equation

$$\rho = \frac{\bar{r}}{0.134(\text{Å})} \tag{26}$$

where $\bar{r} = \sum_{\text{j}}^{\text{all charged species}} x_{\text{j}}'' r_{\text{j}}$ is the mean radius from all charged species in the solution, r_{j} is the radius of ion j, and x_{j}'' is its solvent-free mole fraction. [For example, the value of ρ of a NaCl aqueous solutions is $\rho = (0.5 \times 1.69 + 0.5 \times 2.05)/0.134 = 13.94$, which is close to the value (14.9) used by

Table 1. Summary of the Segment Interaction Energy $\Delta W(\sigma_m,\sigma_n)$ Between Different Types of Segments

No.	Type of Interactions	Sub-Categories	Equation for $\Delta W(\sigma_{\text{m}}^{\text{t}},\sigma_{\text{n}}^{\text{s}})$
1	Non HB–non HB	Non HB–others	26(a)
2	HB–non HB		
3	Ion–non HB		
4	Ionic group–non HB		
5	HB–HB	Donor–donor or acceptor–acceptor	26(a)
		Donor–acceptor	26(b)
6	Ion–ion	Anion–anion	26(c)
		Cation–cation	26(d)
		Anion–cation	26(e)
7	Ion group–ion group	Anionic group–anionic group	26(c)
		Cationic group–cationic group	26(d)
		Anionic group–cationic group	26(f)
8	HB–ion	HB donor–anion	26(g)
		HB donor–cation	26(h)
		HB acceptor–anion	26(i)
		HB acceptor–cation	26(j)
9	HB–ion group	HB donor–anionic group	26(k)
		HB donor–cationic group	26(h)
		HB acceptor–anionic group	26(l)
		HB acceptor–cationic group	26(j)
10	Ion–ion group	Cation–anionic group	26(f)
		Cation–cationic group	26(d)
		Anion–anionic group	26(c)
		Anion–cationic group	26(f)

Table 2. Model Parameters and Their Values

Parameter	Value [kJ/(mol Å^4 e^2)]
A_0	8946.10
B_0	3063.58
A_1	17108.71
A_2	806.06
A_3	430.19
A_4	2214.50
A_5	2246.33
A_6	3386.81
A_7	3624.26
A_8	2071.18
A_9	210.88
B_1	9245.70
B_2	2376.39

Element	Radius (Å)
H	1.30
C	1.83
N	1.83
O	1.72
S	2.16
P	2.12
Li	1.39
Na	1.69
K	2.00
Rb	2.15
Cs	2.34
Mg	1.86
Ca	2.06
Sr	2.18
Ba	2.30
Fe	2.03
Co	1.95
Cu	2.40
Cr	2.22
F	1.33
Cl	2.05
Br	2.167
I	2.319

others[13,17]. The atomic radii used in this work are summarized in Table 2. [Note that many of the element radii (H,C,O,N, S,P,Cl,Br,I) are taken from the literature.[40] Other radii are chosen to be somewhere between the Pauling radius (from X-ray crystallography) and the equilibrium separation distance between the ion and water.[41,42]] The radius of an ionic group (e.g., NO_3^-) is estimated to be that of a sphere having the same surface area as the ionic group, that is, $r_i = \sqrt{A_i/4\pi}$. The ionic strength I_x is determined from Eq. 8 and the activity coefficient from Eq. 10.

The activity coefficient from the COSMO-SAC model

The only input needed for the COSMO-SAC model is the sigma profile of each species in the solution. The detailed procedure of obtaining such a profile can be found elsewhere.[33,37,43,44] Here, we briefly outline the important steps. The equilibrium molecular geometry is determined by minimization of the total energy of the molecule using the quantum mechanical calculation package DMol3.[45] [Note that this step is not needed for monatomic ions.[46]] Then, a solvation calculation in perfect conductor (COSMO)[47] is performed to obtain the screening charges on the molecular surface with all the default settings in DMol3. Note that DMol3 does not allow a calculation of monatomic cations (e.g., Li^+, Na^+, etc.). For such ions, an in-house program[47] is used to determine the screening charges at the ion surface. The sigma-profile of each individual species $p_i^t(\sigma_m^t)$ can then be determined as the histogram of the screening charges. [note that the sigma-profile is normalized, that is, $\sum_t^{\text{nonhb,hb,}\atop\text{ion,iongrp}} \sum_{\sigma_m} p_i^t(\sigma_m) = 1$.]

Figure 2 illustrates the sigma profile for several monatomic cations. It can be seen that the sigma profile of monatomic ions is a delta function centered at a charge density $\sigma = z_i e/4\pi R_i^2$.[46] The sigma profile for a solution is determined from the mole-fraction average of contributions from all the species

$$p_S^t(\sigma_m^t) = \frac{\sum_i x_i A_i p_i^t(\sigma_m^t)}{\sum_i x_i A_i} \tag{27}$$

Once the sigma-profile is available, the segment activity (in both the solution and in the pure species liquid) is

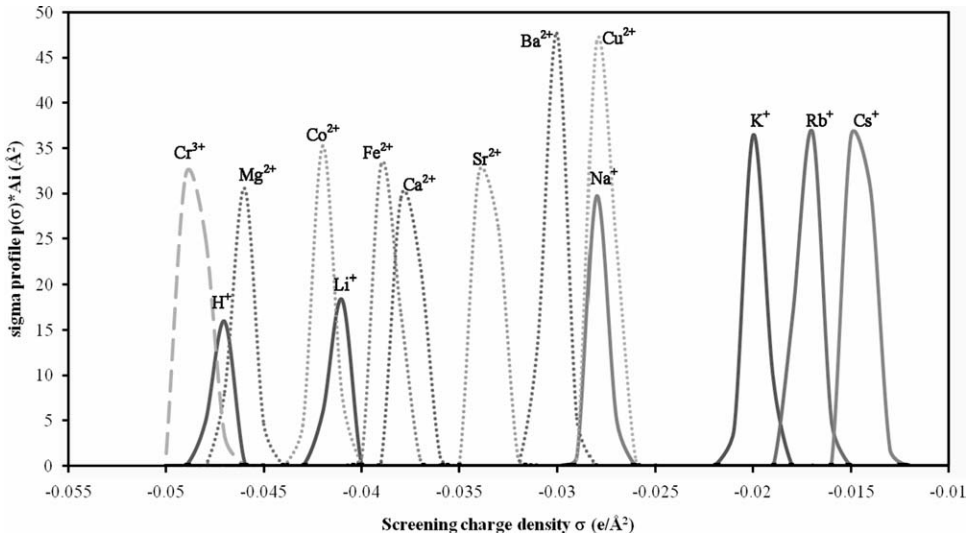

Figure 2. The sigma profile for representative cations.

Table 3. Percent Average Relative Deviation (%ARD) in Mean Activity Coefficient and Water Activity Coefficient Calculation for "Single-Salt, Single-Solvent" Systems at 298.15 K

		Mean Activity Coefficient		Activity Coefficient of Water
		%ARD		%ARD
Electrolyte	Max Molality[a] (mol/kg)	This Work	e-PC SAFT[31]	This Work
		1:1 Monatomic electrolytes		
NaF	1.0	3.88	2.38	0.07
KF	4.0	3.43	3.26	0.24
RbF	3.5	6.08	6.70	–
CsF	3.5	14.58	6.39	–
HCl	6.0	9.00	9.80	0.21
LiCl	4.5	6.58	9.79	0.11
NaCl	6.0	1.23	3.43	0.10
KCl	4.5	0.48	2.38	0.03
RbCl	5.0	0.85	1.35	0.08
CsCl	5.5	1.86	1.91	0.17
NH_4Cl	6.0	1.18	0.95	0.12
HBr	3.0	8.49	9.28	0.07
LiBr	4.5	2.55	3.52	0.09
NaBr	4.0	1.28	1.75	0.07
KBr	5.5	1.43	1.78	0.06
RbBr	5.0	0.59	1.89	0.02
CsBr	5.0	2.09	2.56	0.16
NH4Br	8.0	1.06	6.56	–
HI	3.0	6.61	2.56	0.22
LiI	3.0	5.28	4.49	0.23
NaI	3.5	1.96	1.37	0.12
KI	4.5	3.15	1.44	0.05
RbI	5.0	1.71	3.30	0.06
CsI	3.0	2.12	4.66	0.01
NH_4I	1.1	3.02	2.36	–
		2:1 and 3:1 Monatomic electrolytes		
$MgCl_2$	4.5	7.49	11.08	0.55
$CaCl_2$	5.5	7.31	26.11	1.05
$SrCl_2$	3.5	6.24	11.05	0.18
$BaCl_2$	1.8	3.95	5.68	0.21
$FeCl_2$	2.0	5.05	7.13	0.21
$CuCl_2$	5.0	13.93	19.56	1.55
$CoCl_2$	4.0	15.68	12.10	1.41
$CrCl_3$	1.2	21.44	13.60	0.21
$MgBr_2$	4.5	10.23	13.43	1.08
$CaBr_2$	3.5	5.18	18.31	0.40
$SrBr_2$	2.0	3.68	11.91	0.19
$BaBr_2$	2.0	4.11	6.47	0.24
$CuBr_2$	3.6	20.16	14.32	–
$CoBr_2$	5.0	6.34	8.55	0.56
MgI_2	4.5	18.55	47.18	2.74
CaI_2	2.0	11.67	10.15	0.56
SrI_2	2.0	5.61	11.26	0.30
BaI_2	2.0	5.83	9.46	0.08
CoI_2	5.0	15.41	10.62	3.35
		Hydroxides		
LiOH	4.0	14.4	3.01	–
NaOH	6.0	13.9	6.78	1.93
KOH	6.0	21.23	3.03	3.33
CsOH	1.0	4.84	2.72	0.08
$Ba(OH)_2$	0.2	5.17	2.26	–
		Nitrates		
HNO_3	3.0	7.14	6.87	0.27
$LiNO_3$	6.0	1.74	14.25	0.05
$NaNO_3$	6.0	2.81	1.99	0.13
KNO_3	3.5	6.58	2.28	0.22
$NH4NO_3$	6.0	18.22	29.15	1.72
$RbNO_3$	4.5	9.00	2.92	0.64
$CsNO_3$	1.4	4.87	3.68	0.09
$Mg(NO_3)_2$	4.5	32.06	13.14	4.69
$Ca(NO_3)_2$	6.0	18.43	13.56	3.16
$Sr(NO_3)_2$	4.0	13.13	11.95	0.69
$Ba(NO_3)_2$	0.4	33.95	3.55	0.26

(*Continued*)

Table 3. (Continued)

Electrolyte	Max Molality[a] (mol/kg)	Mean Activity Coefficient %ARD		Activity Coefficient of Water %ARD
		This Work	e-PC SAFT[31]	This Work
$Cu(NO_3)_2$	5.0	24.35	32.96	–
$Co(NO_3)_2$	5.0	4.81	15.92	0.42
$Cr(NO_3)_3$	1.4	7.16	15.48	0.38
		Thiocyanates		
NaSCN	4.0	16.42	2.76	0.86
KSCN	5.0	25.94	1.07	1.82
NH4SCN	2.0	11.94	2.48	–
		Chlorates		
$LiClO_3$	10.0	34.01	11.6	–
$NaClO_3$	3.5	7.77	2.14	0.16
$KClO_3$	0.7	5.31	0.96	0.03
$RbClO_3$	0.3	3.47	0.98	–
$CsClO_3$	0.3	3.24	0.51	–
		Perchlorates		
$HClO_4$	6.0	16.63	9.02	0.71
$LiClO_4$	4.0	2.06	4.13	0.11
$NaClO_4$	6.0	10.25	14.14	0.46
$RbClO_4$	0.3	6.82	5.10	–
NH_4ClO_4	2.1	4.78	7.97	–
$Mg(ClO_4)_2$	1.0	3.04	9.53	0.10
$Ca(ClO_4)_2$	3.0	3.65	17.61	0.33
$Sr(ClO_4)_2$	4.0	9.38	15.91	1.10
$Ba(ClO_4)_2$	5.0	4.30	6.60	0.55
$Cu(ClO_4)_2$	3.0	28.49	25.66	–
$Co(ClO_4)_2$	3.5	9.93	12.65	–
		Bromates		
$NaBrO_3$	2.5	4.66	3.01	0.05
$KBrO_3$	0.5	3.96	1.32	0.02
$RbBrO_3$	0.3	1.94	1.95	–
$CsBrO_3$	0.3	2.84	1.72	–
		Sulfates		
Li_2SO_4	3.0	15.32	20.29	0.81
Na_2SO_4	4.0	14.88	32.63	2.01
K_2SO_4	0.7	17.46	1.61	0.07
Rb_2SO_4	1.8	11.59	11.94	0.57
Cs_2SO_4	1.8	12.77	12.31	0.75
$(NH_4)_2SO_4$	4.0	22.13	17.44	–
$MgSO_4$	3.6	51.71	19.36	0.80
$CuSO_4$	2.0	8.37	12.76	–
$CoSO_4$	2.0	13.10	17.58	–
$Cr_2(SO_4)_3$	1.2	33.58	35.18	0.69
		Phosphates		
Na_2HPO_4	1.25	5.74	11.72	–
K_2HPO_4	1.0	10.29	5.86	–
NaH_2PO_4	6.0	8.98	3.02	0.57
KH_2PO_4	1.8	7.13	2.47	0.14
Overall		9.76	9.12	0.62

[a]Experimental data are taken from Refs. 53 and 54.

determined from Eq. 24, and the residual contribution to the molecular activity coefficient from Eq. 23. The normalize volume r_i and surface area q_i are determined from the molecular volume $r_i = V_i(\text{Å}^3)/(66.694\text{Å}^3)$ and surface area $q_i = A_i(\text{Å}^2)/(79.532\text{Å}^2)$ that can be found in the output file of COSMO calculation. The combinatorial contribution to the activity coefficient calculated from Eq. 21 is combined with the residual contribution (Eq. 19) to obtain the COSMO-SAC activity coefficient.

Property calculations

The Mean Activity Coefficient. The reference state used for charged species in PDH (infinite dilution) and COSMO-SAC (pure fluid) are different. Therefore, special attention is needed when combining these two contributions. The reference state for the activity coefficient from COSMO-SAC is changed from pure fluid to infinite dilution according to the following equation

$$\gamma_i^{*\text{COSMOSAC}} = \frac{\gamma_i^{\text{COSMOSAC}}(x)}{\gamma_i^{\text{COSMOSAC}}(x_i = 0)} \tag{28}$$

The result from Eq. 28 is then combined with that from Eq. 10 to obtain the mean activity coefficient

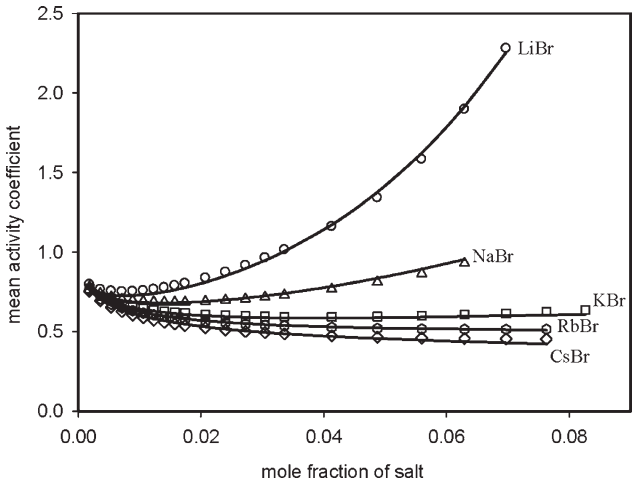

Figure 3. Mean activity coefficient of five 1:1 bromides salts in aqueous solution at 298.15 K.

Solid lines are predictions from this work. Open Symbols represent experimental data.

$$\gamma'_{\pm} = \left(\left(\gamma_{+}^{\mathrm{PDH}} \gamma_{+}^{*\mathrm{COSMOSAC}}\right)^{\upsilon^{+}} \cdot \left(\gamma_{-}^{\mathrm{PDH}} \gamma_{-}^{*\mathrm{COSMOSAC}}\right)^{\upsilon^{-}} \right)^{\frac{1}{(\upsilon^{+}+\upsilon^{-})}} \tag{29}$$

where υ^+ and υ^- are the stoichiometric coefficients of the cation and anion, respectively. Finally, since reported experimental data for the mean activity coefficient are in a molarity scale, it is necessary to convert the concentration scale from mole fraction to molarity as follows[48]

$$\gamma_{\pm} = \frac{1}{1 + \frac{M_s}{1000}(\upsilon^{+} + \upsilon^{-}) m_{\mathrm{mx}}} \gamma'_{\pm} \tag{30}$$

where m_{mx} is the molarity of salt.

The Osmotic Coefficient. The osmotic coefficient ϕ can be obtained from the activity coefficient of the solvent

Table 4. The Degree of Dissociation for Some Representative Aqueous Electrolyte Solutions at Different Concentration Conditions at 298.15 K

Molarity (mol/L)	NaCl	KCl	$BaCl_2$	$LaCl_3$
0.1	0.84	0.86	0.70	0.60
1.0	0.68	0.75	0.49	0.35

The degree of dissociation is calculated from the measured conductivity[53] as $\alpha = \frac{\Lambda}{\Lambda^{\circ}}$, where Λ is molar conductivity and Λ° is the molar conductivity at infinite dilution.[55]

$$\phi = -\frac{x_{\mathrm{S}}}{1 - x_{\mathrm{S}}} \ln(x_{\mathrm{S}} \gamma_{\mathrm{S}}) \tag{31}$$

where x_s and γ_s are the mole fraction and activity coefficient of the solvent, respectively. Note that the activity coefficient for the solvent is determined from Eq. 6 without the need of changing reference state and concentration scale.

The Vapor Pressure. The vapor pressure P^{vap} can also be acquired from the activity of the solvent

$$P^{\mathrm{vap}} = P^{\mathrm{sat}}(T) \cdot x_{\mathrm{S}} \gamma_{\mathrm{S}} \tag{32}$$

where $P^{\mathrm{sat}}(T)$ is the saturated vapor pressure of the solvent at temperature T.

Optimization of model parameters

The value of two of the model parameters (a_0 and b_0 in Table 2) are taken from the literature.[33] The other 11 parameters (a_1 to a_9, b_1 and b_2 in Table 2) and some the element radii (for Mg, Ca, Sr, Ba, Fe, Co, Cu, Cr, F) are obtained by minimizing the following object function:

$$\mathrm{OBJ} = \mathrm{RMS}_{1:1\_\mathrm{monoatomic\_electrolytes}} \cdot 2.0 + \mathrm{RMS}_{2:1,3:1\_\mathrm{monoatomic\_electrolytes,ionic\_groups}} \cdot 1.0 \tag{33}$$

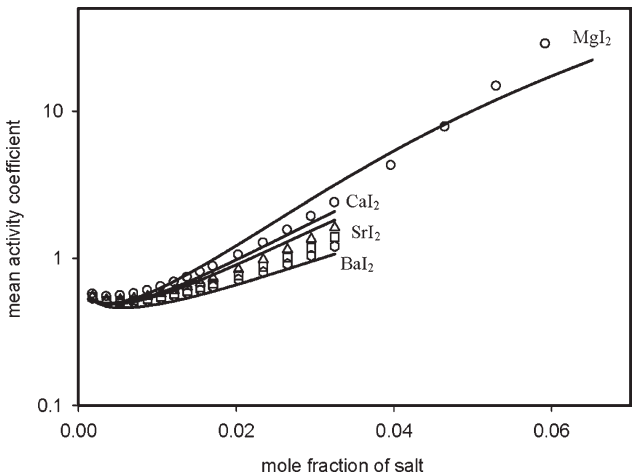

Figure 4. Mean activity coefficient of five 2:1 iodine salts in aqueous solution at 298.15 K.

Solid lines are predictions from this work. Open Symbols represent experimental data.

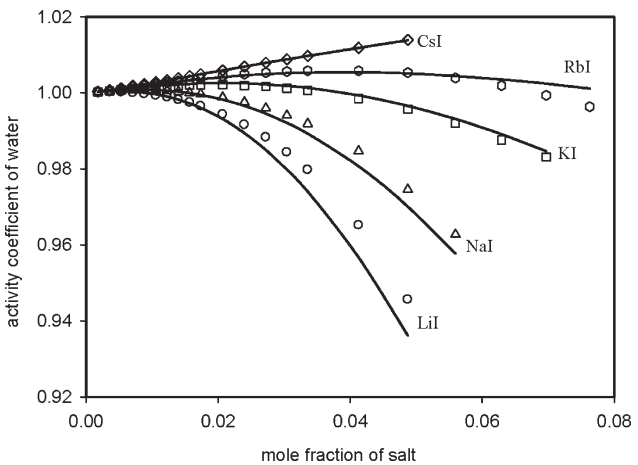

Figure 5. Water activity coefficient of five 1:1 iodide salt in aqueous solution at 298.15 K.

Solid lines are predictions from this work. Open Symbols represent experimental data.

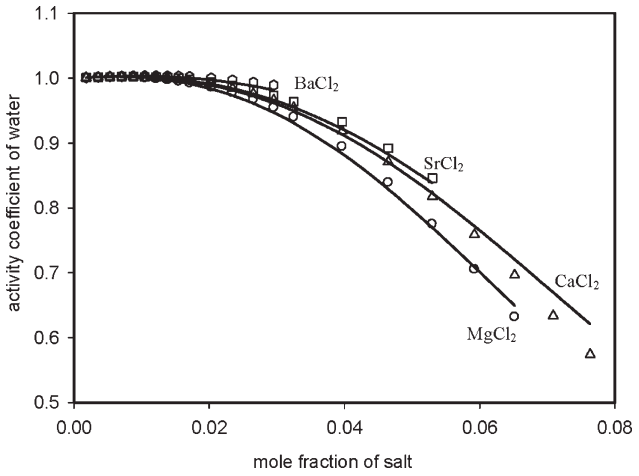

Figure 6. Water activity coefficient of five 2:1 chloride salts in aqueous solution at 298.15 K.

Solid lines are predictions from this work. Open Symbols represent experimental data.

where RMS $= \sqrt{\frac{\sum_{i=1}^{n}\left[\ln\left(\gamma_{i,cal}/\gamma_{i,exp}\right)\right]^2}{n}}$, n is the total number of data points used. The universal parameters used in this new activity model are only optimized for the "single salt, single solvent" systems at 298.15 K (i.e., all the systems listed in Table 3). The parameter optimization proceeded as follows. The radius of each of the monatomic ions is set to be the average of the Pauling radius and the equilibrium separation distance between the ion and water.[41,42] The experimental data of 1:1 electrolytes are used to obtain the initial values of parameters a_1, a_2, a_3, a_5, a_6, a_7, b_1, and b_2. These parameters are further optimized with the inclusion of data of 2:1 and 3:1 electrolytes. Next, the radii of multivalent cations are fine tuned with the values of the eight interaction parameters kept unchanged. Finally, the remaining three parameters (a_4, a_8, and a_9) are fitted to experimental data of electrolytes containing polyatomic ions. The Simplex downhill algorithm[49]

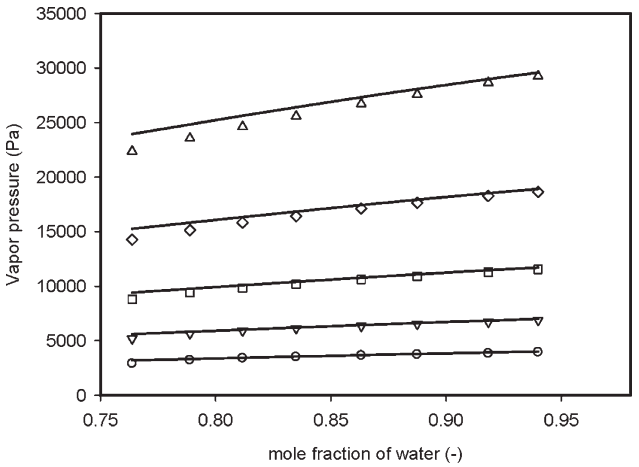

Figure 7. Vapor pressure of cesium chloride in aqueous solution at different temperatures.

Solid lines are predictions from this work. Open Symbols represent experimental data.

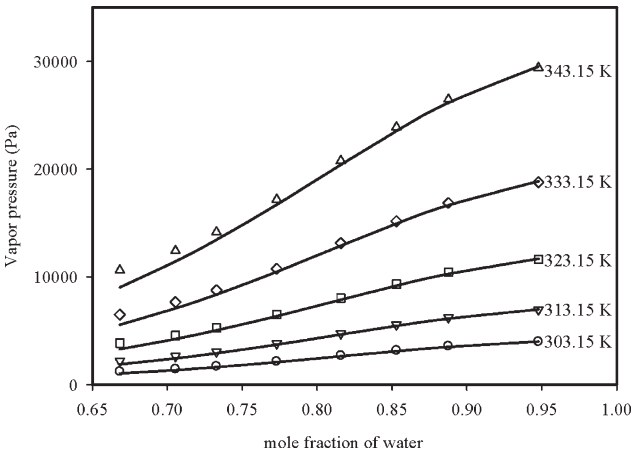

Figure 8. Vapor pressure of calcium dichloride in aqueous solution at different temperatures.

Solid lines are predictions from this work. Open Symbols represent experimental data.

is used for the parameter optimization. Multiple initial guesses for the parameters were examined during the parameterization to avoid being trapped within a local minimum.

Results and Discussion

The proposed method is used to study the following three types of aqueous electrolyte systems

1 single-salt, single-solvent
2 mixed-salt, single-solvent
3 single-salt, mixed-solvent

All the calculations are done using the same set of model parameters, as listed in Table 2.

Table 5. Deviation in Vapor Pressure Calculation for "Single-Salt, Single-Solvent" Systems at Different Temperatures

	Vapor Pressure			
Electrolyte	Max Molality (mol/kg)	Data Points	Temperature Range (°C)	%AAD of lnP
NaCl[b]	6.65	65	15–205	1.58
NaBr[a,b]	9.72	81	20–200	2.22
NaI[a,b]	10.00	94	20–200	2.94
KCl[b]	7.55	76	0–200	0.79
KBr[a,b]	8.40	104	60–200	4.57
KI[b]	9.04	63	20–200	3.74
RbCl[a]	6.95	30	30–70	1.53
CsCl[a,b]	5.94	106	25–200	1.74
NH4Cl[b]	7.47	49	10–100	0.96
$MgCl_2$[a,b]	7.00	123	0–200	4.93
$CaCl_2$[a,b]	9.01	66	20–150	3.76
$CaBr_2$[b]	5.00	43	45–95	3.80
$SrCl_2$[b]	2.10	15	25–100	1.07
$SrBr_2$[a,b]	4.04	55	50–100	1.40
$BaCl_2$[b]	2.06	59	0–200	0.38
$BaBr_2$[a]	3.40	40	30–70	1.09
Overall		1069		2.28

[a]Experimental data are taken from Ref. 56.
[b]Experimental data are taken from Ref. 57.

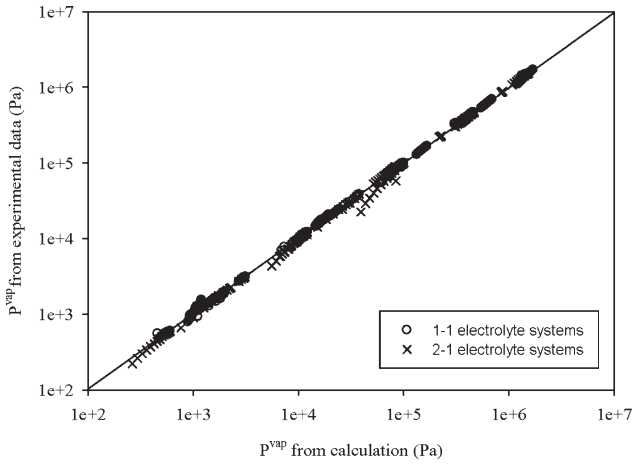

Figure 9. Comparison of predicted and experimental vapor pressure of aqueous electrolyte solutions over a wide range of temperature.

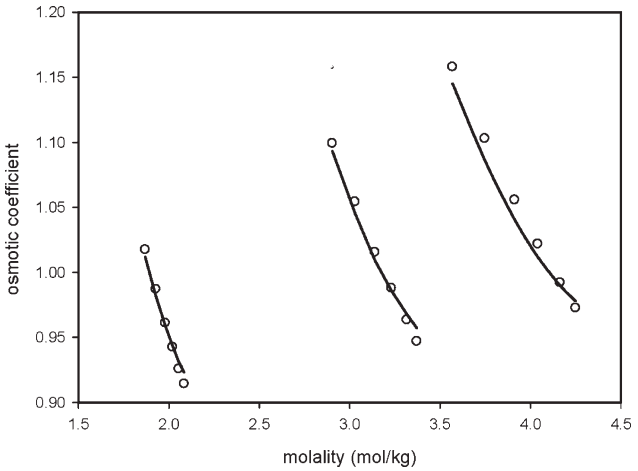

Figure 10. Osmotic coefficient of a mixed-salt system, KCl-NaBr in aqueous solution, at 298.15 K.

Solid lines are predictions from this work. Open Symbols represent experimental data.

Single-salt, single-solvent systems

The experimental data of mean activity coefficient for aqueous solutions containing 1:1 (22 systems, 396 data points), 2:1 (18 systems, 327 data points), 3:1 monatomic electrolytes (1 systems, 11 data points), and aqueous electrolyte solutions with polyatomic ion-groups (59 systems, 985 data points) are used to obtain the 11 universal parameters in the model. The errors in the calculated mean activity coefficient, water activity coefficient are listed in Table 3. The overall percent average relative deviation ($\text{ARD} = \frac{100\%}{n}\sum_{i=1}^{n}\frac{\left|\gamma_i^{\text{cal}}-\gamma_i^{\text{exp}}\right|}{\gamma_i^{\text{exp}}}$) in mean activity coefficient calculations is 9.76%, with that of the 1:1 electrolyte systems being 3.62%, 2:1, 3:1 electrolyte systems 9.89%, and polyatomic ion-groups 12.46%. Figures 3 and 4 illustrate the calculated mean activity coefficient as a function of concentration (solid lines) for some typical electrolytes. Corresponding experimental data (open symbols) are also included for comparison. The results from our model are comparable to a recently published method, e-PC SAFT (also shown in Table 3): Overall ARD 9.12%, 1:1 electrolytes 3.83%, 2:1, 3:1 electrolytes 14.10%, and ionic groups 9.79%. Unlike the e-PC SAFT model where two fitting parameters are needed for each ionic species, the method proposed here does not contain any species dependent variables and is readily applicable to any new electrolyte solution.

The larger value of errors seen in multivalent electrolytes may be attributed to the breakdown of fully dissociation approximation, which is a good assumption for low concentrations. As the electrolyte concentration increases, the degree of dissociation of the positive and negative charged species may also decrease. Table 4 lists the degree of dissociation (determined from conductivity measurements) of several electrolytes in water at low (0.1 mol/L) and high (1 mol/L) concentrations. It is evident that the decrease in the degree of dissociation is even more prominent for 2:1 and 3:1 electrolyte systems. We have neglected the presence of undissoiciated electrolytes in our calculations because this would require the knowledge of dissociation constant, which is not the focus of the present work. The especially large

Table 6. Percent Average Absolute Deviation (%ARD) in Osmotic Coefficient Calculation for "Mixed-Salt, Single-Solvent" Systems at 298.15 K

Electrolytes	Data Points	%ARD
NaCl-KCl[a]	6	1.37
NaCl-KBr[a]	12	0.85
KCl-NaBr[a]	18	0.93
NaBr-KBr[a]	18	0.67
KCl-KBr[a]	18	0.49
NaCl-NaBr[a]	12	1.10
KCl-CsCl[b]	35	0.58
NaCl-CsC[c]	42	1.46
Overall	161	0.93

[a]Experimental data are taken from Ref. 58.
[b]Experimental data are taken from Ref. 59.
[c]Experimental data are taken from Ref. 60.

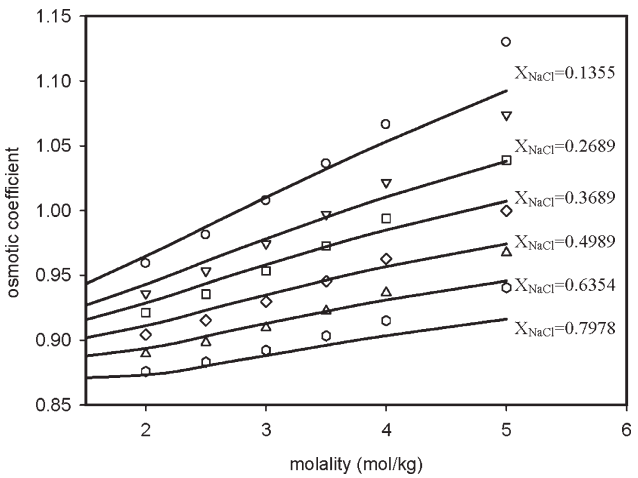

Figure 11. Osmotic coefficient of a mixed-salt system NaCl–CsCl, in aqueous solution, at 298.15 K.

Solid lines are predictions from this work. Open Symbols represent experimental data.

Table 7. Percent Average Absolute Deviations (%ARD) in Mean Activity Coefficient Calculation for "Single-Salt, Mixed-Solvent" Systems at 298.15 K

System[a]	%wt of Non Aqueous Solvent	Data Points	%ARD
KCl-MeOH-Water	10	13	7.92
KCl-MeOH-Water	20	12	12.64
KCl-MeOH-Water	30	14	6.93
KCl-MeOH-Water	40	13	5.92
KCl-MeOH-Water	50	12	4.81
KCl-MeOH-Water	60	12	4.59
KCl-MeOH-Water	70	13	4.54
KCl-MeOH-Water	80	12	2.95
KCl-MeOH-Water	90	10	2.39
Overall		111	5.85
NaCl-EtOH-Water	20	28	1.59
NaCl-EtOH-Water	40	25	2.48
NaCl-EtOH-Water	60	24	3.68
NaCl-EtOH-Water	70	17	3.71
NaCl-EtOH-Water	80	15	9.66
NaCl-EtOH-Water	90	14	9.30
Overall		123	5.07

[a]Experimental data for KCl-MeOH are taken from Ref. 61. Experimental data for NaCl-EtOH are taken from Ref. 62.

deviation found in hydroxides (OH^-) and thiocyanates (SCN^-) is not fully understood. The presence of such a strong base and/or weak acid may significantly alter the proton concentration and cause the formation of ion-solvent complex (the local hydrolysis phenomena),[50] which is not explicitly accounted for in our calculations.

Also, listed in Table 3 are the ARD of the water activity coefficient: Overall 0.62%, 1:1 electrolytes 0.11%, 2:1 and 3:1 electrolytes 0.83%, ionic groups 0.81%. Figures 5 and 6 illustrates water activity coefficient for several typical electrolyte solutions. Although there is a larger deviation in the calculated mean activity coefficient for electrolytes at high concentration and high valence type electrolyte systems, the performance in calculated water activity coefficient is, in general, quite good. The main reason is that solvent (water) is the major part of an aqueous electrolyte solution and the

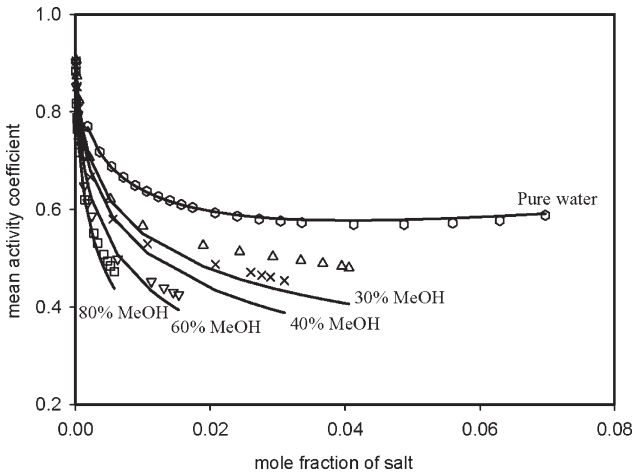

Figure 12. Mean activity coefficient of KCl in methanol–water mixtures at 298.15 K.

Solid lines are predictions from this work. Open Symbols represent experimental data.

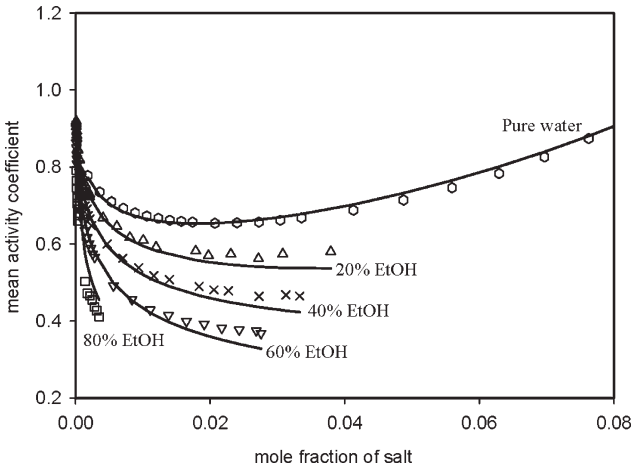

Figure 13. Mean activity coefficient of NaCl in ethanol–water mixtures at 298.15 K.

Solid lines are predictions from this work. Open Symbols represent experimental data.

variation of its activity coefficient with concentration is less sensitive than that of the salt.

The predictions of vapor pressure for aqueous electrolyte solutions at different temperatures for two typical systems are illustrated in Figures 7 (CsCl) and 8 (CaCl2). The AAD in the predicted vapor pressures of 16 systems (from 0 to 205°C, 1069 data points) are listed in Table 5 and shown in Figure 9. The agreement between the predicted and the experimental vapor pressures are very good, with an average absolute deviation in $\ln P^{vap}$ ($\%AAD = \frac{100\%}{n}\sum_{i=1}^{n}\left|\ln\frac{P_i^{vap,cal}}{P_i^{vap,exp}}\right|$) being only 2.28% (or equivalently an ARD of 2.30%). The success in predicting vapor pressure of electrolyte solutions from our model is remarkable since no temperature dependent parameter is used and all the universal parameters were determined using data at 298 K. It is worth noting that some researchers[51,52] use a temperature-dependent hydrated-ion radius in aqueous electrolyte systems to obtain the proper temperature dependence in the mean activity coefficient and the vapor pressure. Our model correctly captures the temperature dependence in the vapor pressure without using temperature-dependent radii.

Mixed-salt, single-solvent systems

The method proposed here is readily applicable to solutions containing two or more salts. The overall ARD (Table 6) in the osmotic coefficient from eight systems (161 data points) is very low, only 0.93%. Therefore, this method produces reliable properties for mixed salt systems.

Figures 10 and 11 illustrate two types of mixed salts systems: with and without a common ion. In Figure 10, the solution, KCl-NaBr-water, contains four ionic species, while in Figure 11 the system, NaCl-CsCl-water, contains a common anion (Cl^-). As can be seen that the method proposed here is capable of describing both types of systems without the need of using any adjustable parameters.

Single-salt, mixed-solvent systems

The overall %ARD in the predicted mean activity coefficient from two mixed-solvent systems, summarized in

Table 7, is slightly larger, around 5%. These results are also shown in Figures 12 and 13. A common feature observed is the underestimation of mean activity coefficient compared to experimental data. Part of the error from our calculation may be a result of the pseudo-single solvent approximation used in the calculation of the long-range effect (the PDH model). (Note that the pseudo-single solvent approximation is not needed is in the COSMO-SAC calculations.) Although the error in our model for the ''single salt, mixed solvents'' system is slightly higher, this model still captures the general behavior of mean activity coefficient with different salt concentration and different ratio between alcohols and water.

Conclusion

In this work, a new activity coefficient model is developed for the prediction of the properties of fully dissociated electrolyte systems. The activity coefficient model contains a long-range part based on the Pitzer-Debye-Huckel theory and a short-range part based on the COSMO-SAC liquid activity coefficient model. The interactions between different types of species, including ions, ionic groups, hydrogen bonding, and non hydrogen bonding, are considered explicitly (with 13 universal parameters). The uniqueness of this approach is that it does not use any ion-solvent pair interaction parameters and does not contain any ion specific parameter other than the element radius.

This model is validated using several representative properties for three types of systems including a single salt in water, mixture salts in water, and a single salt in solvent mixture containing water and alcohols. An excellent agreement with experimental data is obtained for 1:1 electrolyte systems and 1:1 mixed-salt systems. The error in the predictions for systems containing multivalent ions is slightly higher due to the breakdown of fully dissociation approximation used in our calculations. Nonetheless, the accuracy should be satisfactory considering the small amount of universal parameters used. This method provides a variety of properties of, in principle, any electrolyte solutions and is especially useful when no experimental data is available.

Acknowledgments

The authors thank Dr. Chau-Chyun Chen for many useful discussions and valuable comments during the preparation of the manuscript. The financial support from Grant NSC 97-2221-E-002-085 and 98-2221-E-002-087-MY3 by the National Science Council of Taiwan and computation resources from the National Center for High-Performance Computing of Taiwan are acknowledged.

Literature Cited

1. Sandler SI. *Chemical, Biochemical, and Engineering Thermodynamics*, 4th ed. New York: John Wiley & Sons, Inc., 2006.
2. Chen CC. Toward development of activity coefficient models for process and product design of complex chemical systems. *Fluid Phase Equilib.* 2006;241:103–112.
3. Sandler SI. The generalized Van Der Waals partition-function. 1. Basic theory. *Fluid Phase Equilib.* 1985;19:233–257.
4. Abbott MM, Prausnitz JM. Generalized Van Der Waals theory—a classical perspective. *Fluid Phase Equilib.* 1987;37:29–62.
5. Renon H, Prausnit JM. Local compositions in thermodynamic excess functions for liquid mixtures. *Aiche J.* 1968;4:135–144.
6. Abrams DS, Prausnitz JM. Statistical thermodynamics of liquid-mixtures—new expression for excess gibbs energy of partly or completely miscible systems. *Aiche J.* 1975;21:116–128.
7. Fredenslund A, Gmehling J, Michelsen ML, Rasmussen P, Prausnitz JM. Computerized design of multicomponent distillation-columns using Unifac group contribution method for calculation of activity-coefficients. *Ind Eng Chem Process Des Dev.* 1977;16:450–462.
8. Peng DY, Robinson DB. A new two-constant equation of state. *Ind Eng Chem Fundam.* 1976;15:59–64.
9. Chapman WG, Gubbins KE, Jackson G, Radosz M. Saft—equation-of-state solution model for associating fluids. *Fluid Phase Equilib.* 1989;52:31–38.
10. Gross J, Sadowski G. Perturbed-chain saft: an equation of state based on a perturbation theory for chain molecules. *Ind Eng Chem Res.* 2001;40:1244–1260.
11. Pitzer KS. Thermodynamics of electrolytes. 1. Theoretical basis and general equations. *J Phys Chem.* 1973;77:268–277.
12. Lebowitz JL, Percus JK. Mean spherical model for lattice gases with extended hard cores and continuum fluids. *Phys Rev.* 1966;144:251–258.
13. Chen CC, Britt HI, Boston JF, Evans LB. Local composition model for excess Gibbs energy of electrolyte systems. 1. Single solvent, single completely dissociated electrolyte systems. *Aiche J.* 1982;28:588–596.
14. Chen CC, Bokis CP, Mathias P. Segment-based excess gibbs energy model for aqueous organic electrolytes. *Aiche J.* 2001;47:2593–2602.
15. Song YH, Chen CC. Symmetric nonrandom two-liquid segment activity coefficient model for electrolytes. *Ind Eng Chem Res.* 2009;48:5522–5529.
16. Chen CC, Simoni LD, Brennecke JF, Stadtherr MA. Correlation and prediction of phase behavior of organic compounds in ionic liquids using the nonrandom two-liquid segment activity coefficient model. *Ind Eng Chem Res.* 2008;47:7081–7093.
17. Pitzer KS. Electrolytes from dilute-solutions to fused-salts. *J Am Chem Soc.* 1980;102:2902–2906.
18. Lin CL, Lee LS. A two-ionic-parameter approach for ion activity coefficients of aqueous electrolyte solutions. *Fluid Phase Equilib.* 2003;205:69–88.
19. Lin CL, Tseng HC, Lee LS. A three-characteristic-parameter correlation model for strong electrolyte solutions. *Fluid Phase Equilib.* 1998;152:169–185.
20. Mortazavi-Manesh S, Taghikhani V, Ghotbi C. A new model in correlating the activity coefficients of aqueous electrolyte solutions with ion pair formation. *Fluid Phase Equilib.* 2007;261:313–319.
21. Ghotbi C, Vera JH. In extension to mixtures of two robust hard-sphere equations of state satisfying the ordered close-packed limit, 2001. *Can Soc Chem Eng.* 2001;678–686.
22. Jin G, Donohue MD. An equation of state for electrolyte-solutions. 3. Aqueous-solutions containing multiple salts. *Ind Eng Chem Res.* 1991;30:240–248.
23. Jin G, Donohue MD. An equation of state for electrolyte-solutions. 2. Single volatile weak electrolytes in water. *Ind Eng Chem Res.* 1988;27:1737–1743.
24. Jin G, Donohue MD. An equation of state for electrolyte-solutions. 1. Aqueous systems containing strong electrolytes. *Ind Eng Chem Res.* 1988;27:1073–1084.
25. Vimalchand P, Donohue MD. Thermodynamics of quadrupolar molecules—the perturbed-anisotropic-chain theory. *Ind Eng Chem Fundam.* 1985;24:246–257.
26. Henderson D, Blum L. Perturbation-theory for charged hard-spheres. *Mol Phys.* 1980;40:1509–1511.
27. Fürst W, Renon H. Representation of excess properties of electrolyte-solutions using a new equation of state. *Aiche J.* 1993;39:335–343.
28. Schwartzentruber J, Renon H, Watanasiri S. Development of a new cubic equation of state for phase-equilibrium calculations. *Fluid Phase Equilib.* 1989;52:127–134.
29. Myers JA, Sandler SI, Wood RH. An equation of state for electrolyte solutions covering wide ranges of temperature, pressure, and composition. *Ind Eng Chem Res.* 2002;41:3282–3297.
30. Myers JA, Sandler SI, Wood RH, Balashov VN. Ion activities in dilute solutions near the critical point of water. *J Phys Chem B.* 2003;107:10906–10911.
31. Held C, Cameretti LF, Sadowski G. Modeling aqueous electrolyte solutions—Part 1. Fully dissociated electrolytes. *Fluid Phase Equilib.* 2008;270:87–96.
32. Cameretti LF, Sadowski G, Mollerup JM. Modeling of aqueous electrolyte solutions with perturbed-chain statistical associated fluid theory. *Ind Eng Chem Res.* 2005;44:3355–3362.

33. Lin ST, Sandler SI. A priori phase equilibrium prediction from a segment contribution solvation model. *Ind Eng Chem Res*. 2002;41:899–913.
34. Chen CC, Song YH. Generalized electrolyte-Nrtl model for mixed-solvent electrolyte systems. *Aiche J*. 2004;50:1928–1941.
35. Novotny P, Sohnel O. Densities of binary aqueous-solutions of 306 inorganic substances. *J Chem Eng Data*. 1988;33:49–55.
36. Bradley DJ, Pitzer KS. Thermodynamics of electrolytes. 12. Dielectric properties of water and Debye-Huckel parameters to 350-Degrees-C and 1-Kbar. *J Phys Chem*. 1979;83:1599–1603.
37. Lin ST, Chang J, Wang S, Goddard WA, Sandler SI. Prediction of vapor pressures and enthalpies of vaporization using a cosmo solvation model. *J Phys Chem A*. 2004;108:7429–7439.
38. *Project 801, Evaluated Process Design Data, Public Release Documentation, Design Institute for Physical Properties (DIPPR)*, American Institute of Chemical Engineers (AIChE), 2006.
39. Chen CC, Song YH. Extension of nonrandom two-liquid segment activity coefficient model for electrolytes. *Ind Eng Chem Res*. 2005; 44:8909–8921.
40. Klamt A, Jonas V, Burger T, Lohrenz JCW. Refinement and parametrization of Cosmo-Rs. *J Phys Chem A*. 1998;102:5074–5085.
41. Marcus Y. Ionic-radii in aqueous-solutions. *Chem Rev*. 1988;88: 1475–1498.
42. Satheesan Babu C, Lim C. A new interpretation of the effective born radius from simulation and experiment. *Chem Phys Lett*. 1999; 310:225–228.
43. Hsieh C-M, Lin S-T. First principle predictions of vapor-liquid equilibria for pure and mixture fluids from the combined use of cubic equations of state and solvation calculations. *Ind Eng Chem Res*. 2009;48:3197–3205.
44. Hsieh CM, Lin ST. Determination of cubic equation of state parameters for pure fluids from first principle solvation calculations. *Aiche J*. 2008;54:2174–2181.
45. Delley B. An All-Electron Numerical-Method for Solving the Local Density Functional for Polyatomic-Molecules. *J. Chem. Phys*. 1990; 92:508–517. DMOL3 is available from Accelrys, Inc. as part of Materials Studio and the Cerius2 program suites.
46. Lin ST, Hsieh CM. Efficient and accurate solvation energy calculation from polarizable continuum models. *J Chem Phys*. 2006;125.
47. Klamt A. Conductor-like screening model for real solvents—a new approach to the quantitative calculation of solvation phenomena. *J Phys Chem*. 1995;99:2224–2235.
48. Prausnitz JM, Lichtenthaler RN, Azevedo EGd. *Molecular Thermodynamics of Fluid-Phase Equilibria*, 3rd ed. Taipei: Pearson Education Taiwan Ltd., 1999.
49. Press WH, Flannery BP, Teukolsky SA, Vetterling WT. *Numerical Recipes—The Art of Scientific Computing*. New York: Cambridge, 1986.
50. Robinson RA, Harned HS. Some aspects of the thermodynamics of strong electrolytes from electromotive force and vapor pressure measurements. *Chem Rev*. 1941;28:419–476.
51. Papaiconomou N, Simonin JP, Bernard O, Kunz W. Description of vapor-liquid equilibria for Co_2 in electrolyte solutions using the mean spherical approximation. *J Phys Chem B*. 2003;107:5948–5957.
52. Simonin JP, Bernard O, Papaiconomou N, Kunz W. Description of dilution enthalpies and heat capacities for aqueous solutions within the Msa-Nrtl model with ion solvation. *Fluid Phase Equilib*. 2008; 264:211–219.
53. Robinson RA, Stokes RH. *Electrolyte Solutions*, 2nd ed. Oxford: Butter-worth, 1970.
54. Lobo VMM, Quaresma JL. *Handbook of Electrolyte Solutions, Parts A and B*. Amsterdam: Elsevier, 1989.
55. Laidler KJ. *Physical Chemistry*. Boston: Houghton Mifflin, 2003.
56. Zaytsev ID, Aseyev GG. *Properties of Aqueous Solutions of Electrolytes*. Boca Raton: CRC press, Inc. 1992.
57. Patil KR, Tripathi AD, Pathak G, Katti SS. Thermodynamic properties of aqueous-electrolyte solutions. 2. Vapor-pressure of aqueous-solutions of Nabr, Nai, Kci, Kbr, Ki, Rbcl, Cscl, Csbr, Csi, Mgcl2, Cacl2, Cabr2, Cai2, Srcl2, Srbr2, Sri2, Bacl2, and Babr2. *J Chem Eng Data*. 1991;36:225–230.
58. Covingto AK, Lilley TH, Robinson RA. Excess free energies of aqueous mixtures of some alkali metal halide salt pairs. *J Phys Chem*. 1968;72:2759–2763.
59. Robinson RA. The osmotic properties of aqueous caesium chloride+potassium chloride and caesium chloride+lithium chloride mixtures at 25-degrees-c. *Trans Faraday Soc*. 1953;49:1147–1149.
60. Robinson RA. The osmotic properties of aqueous sodium chloride cesium chloride mixtures at 25-degrees. *J Am Chem Soc*. 1952;74: 6035–6036.
61. Malahias L, Popovych O. Activity-coefficients and transfer free-energies of kcl in methanol-water solvents at 25-degrees-c. *J Chem Eng Data*. 1982;27:105–109.
62. Esteso MA, Gonzalezdiaz OM, Hernandezluis FF, Fernandezmerida L. Activity-coefficients for Nacl in ethanol-water mixtures at 25-degrees-c. *J Sol Chem*. 1989;18:277–288.

Manuscript received Aug. 1, 2009, revision received Apr. 12, 2010, and final revision received Jun. 4, 2010.